Structural and compositional properties of the PbS-Si heterojunction

H. Elabd and A. J. Steckl
Rensselaer Polytechnic Institute, Troy, New York 12181

(Received 16 April 1979; accepted for publication 10 August 1979)

The physical and chemical structure of thin-film PbS deposited from chemical solution on monocrystalline Si substrate was studied by electron microscopy, x-ray diffraction, and Auger electron spectroscopy. The as-grown PbS has been found to consist of a uniform polycrystalline film. The crystallite size and orientation were found to depend on the orientation of the substrate and were observed to vary between 0.25 and 0.4 μm. Low-temperature treatment of the PbS film was found to be an effective method for revealing the film structure, without altering the grain size. A secondary PbS macrostructure consisting of isolated chainlike clusters was found to coexist with the thin film. The dimensions of the clusters were generally up to an order of magnitude larger ($\sim$3–5 μm) than the thickness of the film (0.5 μm). The microstructure of the cluster was found to be similar to that of the film, consisting of crystallites of the same size. The chemical structure of the PbS film and of the PbS-Si interface was investigated by Auger electron spectroscopy in conjunction with argon ion sputtering. Chemical depth profiles indicate a PbS film of uniform composition. No major contaminants were observed in the bulk of the film. A peak in oxygen content was found to exist at the PbS-Si interface and at the surface of the PbS film. Heat treatment in air increased the oxygen peaks substantially and reduced the sulfur concentration at the film surface.

PACS numbers: 81.15.Lm, 61.16.Di, 68.60. + q, 81.40. − z

I. INTRODUCTION

Recent studies have shown that the lead sulfide–silicon heterojunction, PbS-Si HJ, formed by solution-grown polycrystalline PbS film on single-crystal silicon, exhibits substantial ir sensitivity,[1–3] whereas evaporated polycrystalline PbS films on Si exhibit no significant photovoltaic response.[4] The use of the PbS-Si HJ has been recently proposed as an approach to the realization of large-scale ir focal plane array integration.[5] Hence, a study of the structure and composition of the PbS-Si HJ was performed to evaluate some of its fundamental properties which would shed more light on the operation of the junction as an ir detector.

Several authors have prepared and investigated the utilization of PbS–wide-band-gap semiconductor heterojunctions as sensitive infrared photodetectors. Heterojunctions of Ge-PbS,[6–8] GaAs-PbS,[9,10] CdS-PbS,[11,12] and Si-PbS [8,13–15] have been prepared from a high-pH aqueous solution of thiourea and lead nitrate at room temperature.

The PbS and Si systems differ in their crystal structure, chemical bonding, lattice constant, and thermal properties. PbS crystallizes in a NaCl structure, whereas Si crystallizes in the diamond structure. The Si bond is covalent with tetrahedral coordination, whereas the PbS bond is a mixture of covalent and ionic bonds with octohedral coordination.

The lattice constant of the PbS crystal (5.9356 Å) is significantly larger than that of silicon (5.43086 Å), resulting in a lattice mismatch of roughly 8.88%. The linear expansion coefficient of PbS (18.73×10^{-6}/°C) is six times larger than that of Si (3×10^{-6}/°C). Consequently, large stresses result when the PbS-Si HJ is operated at low temperature. For example, the force of thermoelastic stresses in PbS caused by a 100 °C change in temperature is approximately 20 kg_f /mm^2, which is far beyond the yield point of PbS. Hence, plastic deformation can occur due to either heating or cooling of the heterojunction, and the thermal stresses are released by slip along dislocations and grain boundaries.

The fabrication of the PbS-Si HJ by liquid chemical deposition is discussed in Sec. II. The microstructure of the PbS film and the crystallite orientation were studied by scanning electron microscopy (SEM) and x-ray diffraction. The results of that study are presented in Sec. III. The study of the chemical composition by x-ray and Auger electron spectroscopy (AES) analysis is presented in Sec. IV.

II. SAMPLE PREPARATION

A. Chemical-solution growth method

The PbS-Si HJ is formed by growing, at room temperature, a PbS film from chemical solution[6,13,15] onto a silicon substrate. The constituents of the growth solution are lead nitrate, $Pb(NO_3)_2$ (0.175M), soldium hydroxide, NaOH (0.57M), thiourea, $(NH_2)_2CS$ (1.0M), and DI water. The mixing ratio is 1 : 3 : 1 : 12.5 parts in the solution. The NaOH molar solution is prepared by titration. This growth process results in a PbS film in intimate and continuous contact with the silicon substrate, as was verified under the SEM and by AES analysis.

AES and SEM samples were prepared by depositing a thin PbS film on 1×1-cm^2 Si substrates with (100) and (111) orientations, or on glass substrates. The heterostructures were treated under various conditions prior to SEM or AES analysis.

The deposition of the PbS film was preceded by substrate cleaning and the removal of organic and inorganic contaminants. The procedure suggested by Kern and Puotinen,[16] based on hydrogen peroxide solutions at high pH, was found to be very effective. Silicon substrates were also etched, prior to film deposition, by a mixture of one part 40% HF, two parts 70% HNO_3, and two parts 99.8% acetic

 0021-8979/80/010726-12$01.10

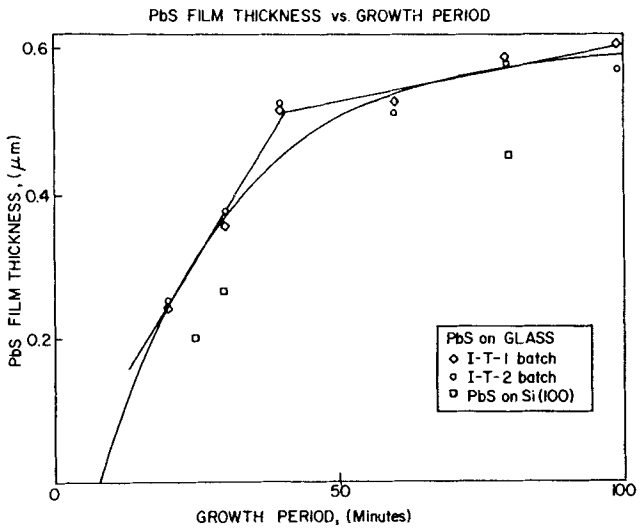

FIG. 1. PbS film thickness versus growth period.

acid. The samples were then transfered to a Si oxide etch bath and a subsequent water bath. The samples were kept in a DI water bath during the brief period required to mix the growth solution to avoid exposing the Si wafer to air. The high-*pH* growth solution dissolves during the initial growth phase any silicon oxide[17] remaining on the surface of the substrate. The *pH* of the growth solution was measured using a full-range glass electrode and was corrected for sodium ion error. The *pH* value is 13 at the beginning of the reaction and drops to almost 12.5 during the first half hour of the reaction.

The chemical reaction involved in the PbS deposition is not well understood and several side reactions may be occuring simultaneously with the PbS deposition reaction. It is proposed that the following chemical reaction is taking place:

$$Pb(NO_3)_2 + (NH_2)_2CS + 4NaOH \rightarrow Na_2Co_3 + 2NH_3 + PbS + NaNO_3 + H_2O\,.$$

NaOH is consumed during the reaction as well as reacting with CO_2 in air and consequently a drop in the *pH* would be expected, as experimentally observed.

Kicinski[18] studied PbS deposition by the reaction of lead acetate, thiourea, and sodium hydroxide. He proposed that the reaction of lead acetate with thiourea forms a complex salt, which will in turn decompose to deposit PbS with by-products of lead carbonate and ammonia. The details of the chemical reaction of lead nitrate with thiourea and sodium hydroxide were not studied previously, but they are thought to be similar.

B. Growth rate and thickness measurements

The term "film thickness" as used in the present discussion refers to the average thickness of the film. Film thickness as measured by different techniques may differ due to experimental error of the measurement and the presence of relatively large chainlike clusters on the surface of the film. These cluster formations are not uniformly distributed across each section of the film and are also nonuniform in height. Hence, evaluation of the thickness by the SEM or by a profilmometer yield best results only after averaging between several sections of the film.

The problem of thickness evaluation of PbS films, for various types of measurements, was encountered earlier,[19] and solved by choosing an average best estimate for the thickness of a PbS layer. The average film thickness was determined by the gravimetric method, with an assumed PbS film density of 7.5 g/cm^3.

Figure 1 shows the PbS film thickness versus growth

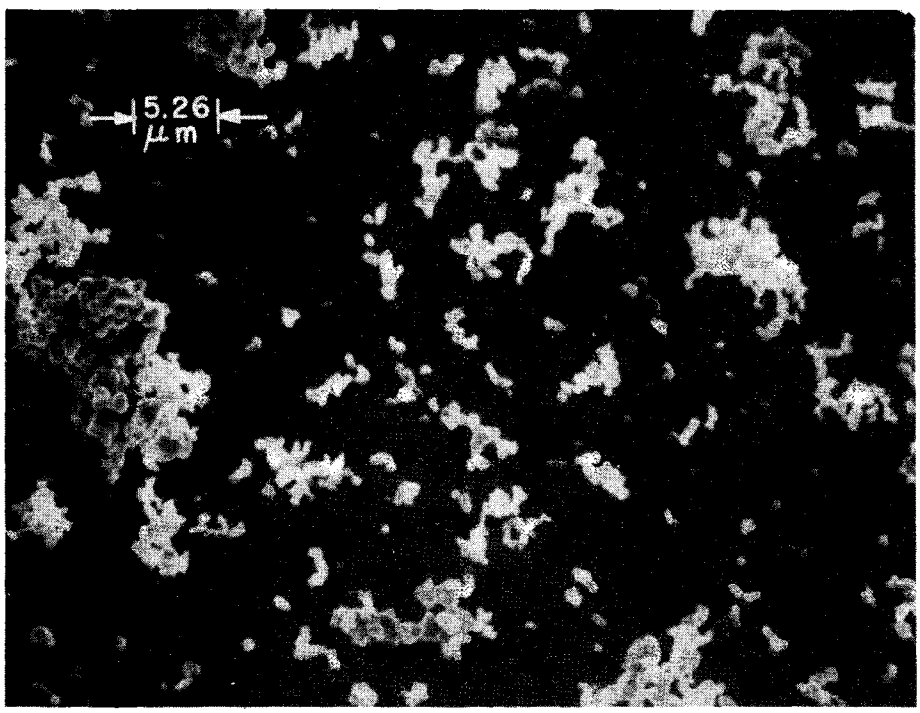

FIG. 2. PbS film surface morphology, (100) Si substrate, $t = 6000$ Å.

period. The batches of glass substrates containing six slices each, and three silicon substrates were used to evaluate the average film thickness as the growth period was altered. The average film thickness grown on the glass substrates of the first batch, I-T-1, was found to be very close to that of the second batch, I-T-2. T is the growth period (20, 30, 40, 60, 80, 100 minutes), for different samples. Average film thickness grown on (100) silicon substrates was found to be up to 20% less that that grown on glass. The difference in the surface roughness and structure of the substrates alters the amount of PbS precipitated.

The growth rate in the first hour averages 60–80 Å/min at room temperature. The film growth saturates after 80 min and very little growth occurs thereafter. The saturation is due to the consumption of available Pb and S ions in the mixture. The data in Fig. 1 closely resembles the results[20] obtained from the plumbite-thiourea reaction. An accurate measurement of the film thickness with an interferometer was difficult because of the lack of a sharp edge on the film. This edge could not be produced by either chemical etching or laser delineation.

C. Surface topology

The surface topology of the PbS films was examined with a scanning electron microscope. The as-grown PbS film had a generally smooth appearance under the SEM and no grain boundaries were immediately visible. Figure 2 shows an SEM photograph of a PbS film grown on (100) silicon. The surface of this PbS film appears to be generally smooth, but with dense concentrations of clusters that vary from 1 to 10 μm in size. The photograph is obtained in the secondary electron mode.

In an attempt to understand the origin of the clusters, the growth solution was filtered using filters with a pore size of 0.22 μm (Millipore Corp.). SEM analysis clearly shows the presence of clusters in the growth solution even at early stages of the reaction. The formation of clusters in the chemical solution itself can be due to nucleation around impurity molecules. The surface of silicon substrates was investigated by SEM prior to PbS deposition. In general, the surface was smooth and only a few carbon and other impurity particles could be seen.

The cluster size as estimated from SEM photographs is between 1 and 10 μm in width (laterally) and 1–6 μm in height.

III. PbS FILM MICROSTRUCTURE

Precipitation of thin PbS films onto solid substrates from aqueous alkaline solution has been used in industry and by many researchers to form photoconductive detectors.[21] However, most of the published literature discusses only briefly the structure and orientation of the films. The surface of the as-grown PbS film, shown in Sec. II C does not reveal the shape and size of the grains or crystallites of the PbS. It is common practice to chemically or thermally etch away the top few atom layers of a specimen to reveal the more representative structure underneath. In this section the results of a study of the structure of PbS layers are presented. The investigation employed x-ray and SEM analyses.

The scanning electron microscope, AMR 1000, was used to examine the PbS films grown on Si and glass substrates. The SEM is equipped with x-ray detection equipment and a minicomputer programmed to analyze and display the energy spectrum of x-ray lines from elements detected within the electron-beam spot. In effect it functions as an energy dispersive spectrometer (EDS). The two basic SEM imaging techniques used, the backscattered electron mode and secondary electron mode, are described in detail elsewhere.[22]

PbS films grown on Si and glass substrates were examined under the SEM with and without uniform complete gold film coverage (shadowing). The microstructure revealed is basically the same in all cases. Gold shadowing was found to be effective in reducing charge-up and improving image quality. On some samples, Latex spheres 0.481 μm in diameter were used to calibrate the grain size. In some of the SEM samples the PbS film grown on silicon was sputter

TABLE I. Chemical etch of PbS films on Si and glass substrates.

Etchant	Temp. (°C)	Observed effects
Concentrated HBr (Ref. 28)	22	Dissolves PbS film grown on Si and glass immediately upon contact without staining Si surface
Concentrated HI (Ref. 28)	22	The same effect as above
30 parts HCl, 10 parts HNO_3 +1 part acetic acid (Refs. 24 and 27)	50	Decomposes PbS film grown on Si and glass substrates, leaving the Si surface partially stained
Concentrated HNO_3 (Ref. 24)	70	The same effect as above
HBr and DI water in 1 : 10 volume ratio (and several other concentrations)	22	This etch reveals a network of cracks and circular etch pits in PbS grown on glass after 1–4 min of the beginning of the reaction, the PbS film lifts off the substrate in 5 min and floats on the surface of the etchant
KOH and NaOH, 0.6 M	22	Marked increase in the surface roughness after 1–2 min followed by film separation from the substrate

TABLE II. Tabulation of various estimates of the average grain size in 4000 Å PbS films.

Substrate	Mean crystallite dimension x-ray diffraction (Å)	SEM estimate of grain size (Å) $A \approx B$
Si(100)	3430	3400–3800
Si(111)	1850	1500–2000
Glass[a]	2020	1400–2700

[a]Grain size of PbS-glass reported here compares closely to that reported by G.W. Mahlman, [Phys. Rev. **103**, 6 (1956)].

etched to produce a step in the film, thus enabling the investigation of the interface and microstructure.

A. Chemical and thermal etching characteristics

Chemical etching is the most common method used to reveal grain boundaries and defects on crystalline surface. Previous work[23–26] has dealt with the use of selective etchants in revealing dislocations in the PbS crystals. Early experiments[27] revealed that hydrobromic acid (HBr) and hydriodic acid (HI) were the best etchants for PbS films grown on Si and glass substrates. It was experimentally verified that repeated use of these acids does not result in staining the silicon surface. Hence HBr and HI either do not react with Si or the reaction rate is negligibly small. The reaction of concentrated HBr with PbS films releases gaseous by-products with the strong and distinct smell of hydrogen sulfide, H_2S.

Due to lift-off of the PbS film, chemical etches were unable to reveal the crystalline structure of the film, although considerable increase in the surface roughness was noticed prior to film-substrate separation.

Different chemical etchants were used on the PbS film surface either to remove the PbS film off the Si surface or to reveal the microstructure of the film. The etchants, temperature of the reaction, and the observed effects are summarized in Table I.

Thermal etching or faceting is the process of altering the surface structure by heating in a gaseous environment. The substructure revealed by thermal etching has direct relationship to the crystal structure as opposed to the more complex relationship in the case of chemical etching.[28] The thermal faceting of PbS films on Si and glass substrates was conducted by heating at different temperatures in air. It was found that, even at very low temperatures compared to the melting point of PbS (1117 °C), grooves form at the grain boundaries and the surface structure is revealed. The PbS grains (crystallites) are seen to be orthorhombic in structure ($a \cong b \neq c$ and all angles $\cong 90°$). The grain size of the PbS film grown on monocrystalline (100) Si and glass substrates has been estimated from SEM photographs taken with $100K \times$ and $50K \times$ magnifications and by comparison to latex spheres 0.481 μm in diameter. The SEM estimate of the grain size is compared to the mean crystallite dimension computed from x-ray diffraction data in Table II.

SEM micrographs of the thermally etched PbS surface suggest that the grains have random orientation with respect to each other except that the larger grain dimensions, a and b, are generally parallel to the surface of the substrate and the smallest dimension, c, is roughly normal to the surface.

The grains vary in size with the substrate, ranging from ~1750 Å for Si (111) to ~3600 Å for Si (100). By comparison, the range of crystallite size of lead salt films reported in the literature varies from 100 Å to 2 μm depending on the method of preparation. For chemical deposition by the basic reaction between thiourea and lead acetate, the grain size

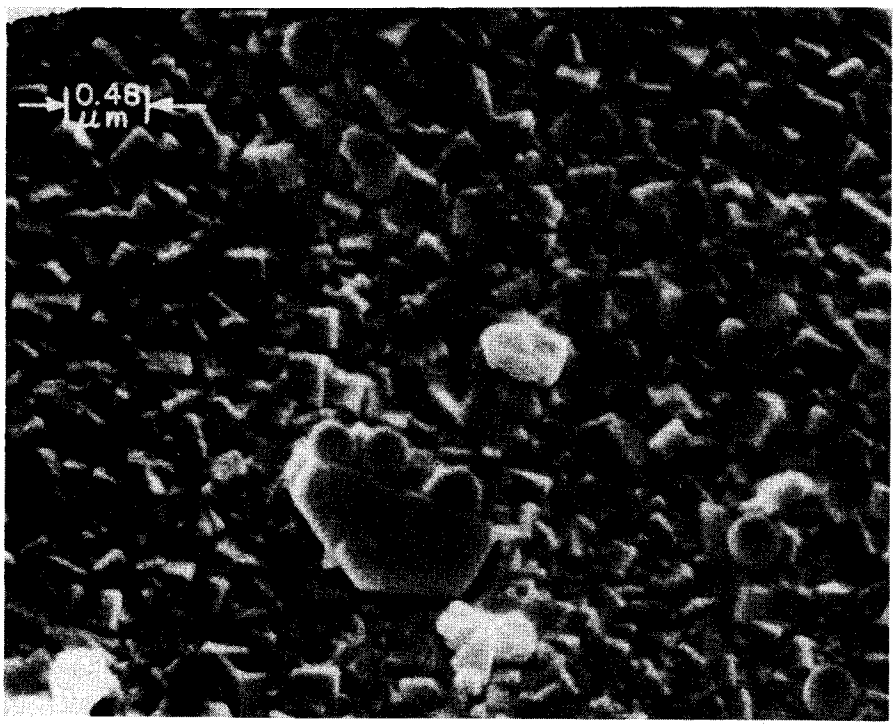

FIG. 3. Surface of PbS film grown on (100) Si, after thermal etching for 20 h at 200 °C. (Latex sphere diameter = 0.481 μm).

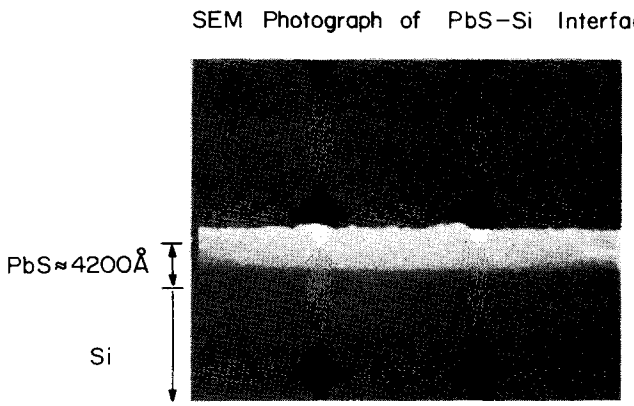

FIG. 4. PbS-(100) Si heterostructure cross-section.

reported ranges from 1000 Å to 1 μm.[21] The average grain size in PbS layers grown on Si (100) is 3600Å. This is considerably larger than the average grain size in PbS layers grown on glass, 2000 Å. Figure 3 shows the surface of PbS grown on Si (100) after thermal etching for 20 h at 200 °C. Latex spheres of 0.481 μm diameter are used for scale calibration. The large rectangular-shaped structures have apparently been introduced from the solution containing the latex spheres since they have not been observed on PbS films prior to the application of the Latex solution.

No significant grain growth occurred with variations in the thermal etching period or temperature. The grain size of PbS film grown on a (100) Si substrate as evaluated from SEM photographs after thermal etching for 20 and 35 h at 200 °C and 66 h at 500 °C is roughly constant. The cross section of a PbS film grown on (100) silicon is shown in Fig. 4. The film thickness is 4200 Å and thickness variation in this cross section is about 10%.

Figures 5 and 6 show an 8000-Å PbS film deposited on a 2000-Å layer of SiO_2. After deposition the structure was sputter etched through a metal mask. In Fig. 5 the edge of the PbS film is in the foreground, while in Fig. 6 the edge appears in the background. Two well-defined structures are evident in addition to the film itself: clusters and spikes. It will be shown that the clusters are composed of the same crystallites as the film. The spikes, appearing in front of the PbS film edge, are known to develop[22] in SEM images of surfaces that are eroded by ion bombardment. They can be caused by shielding particles on the surface, inclusions, or they may occur along slip lines. Some hillocks have been observed on the thermally oxidized Si surface and consequently also in the PbS grown on top. Hillocks rises and falls during temperature cycling of thin Al film on oxidized Si substrate has been reported in the literature,[22] and is caused by mechanical stresses due to thermal expansion in multilayer structure.

In Fig. 6, the remainder of a cluster is shown surrounded by the spikes on the Si surface. The cluster is clearly seen to originate at the level of the PbS-Si interface. Clusters accompany the growth of PbS on glass, SiO_2, and Si substrates and are the main source of surface irregularity in the PbS films.

Thermal etching was also seen to delineate the microstructure of the clusters. Figure 7 shows a cluster after thermal etching at 200 °C for 20 h. The as-grown cluster, as seen in Fig. 6, consist of smooth spherical conglomerates. After

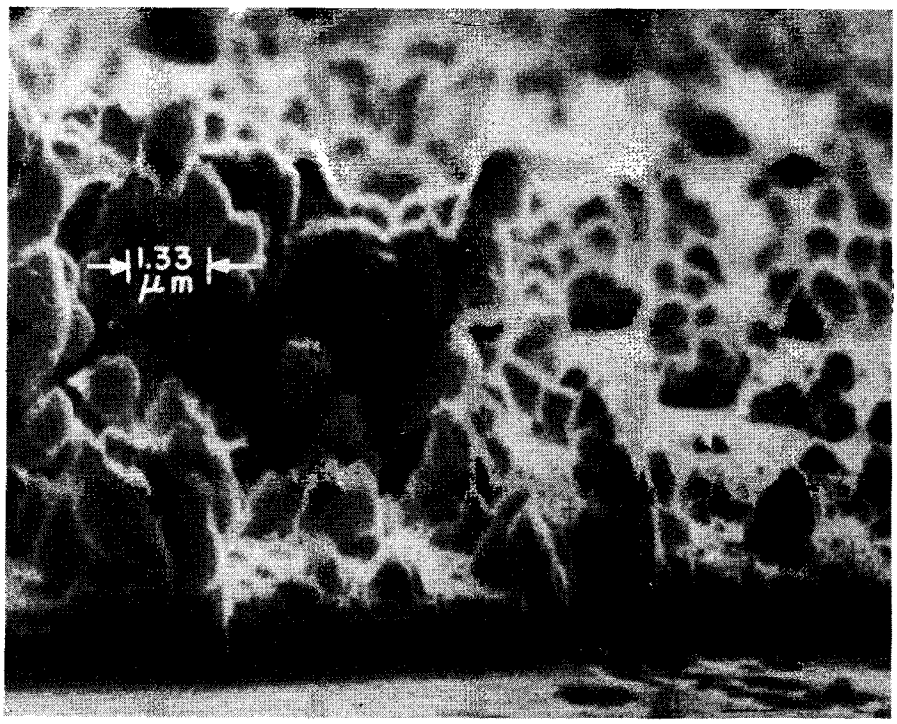

FIG. 5. Sputter-etched PbS film on SiO_2–(100) Si (tilt angle:60°).

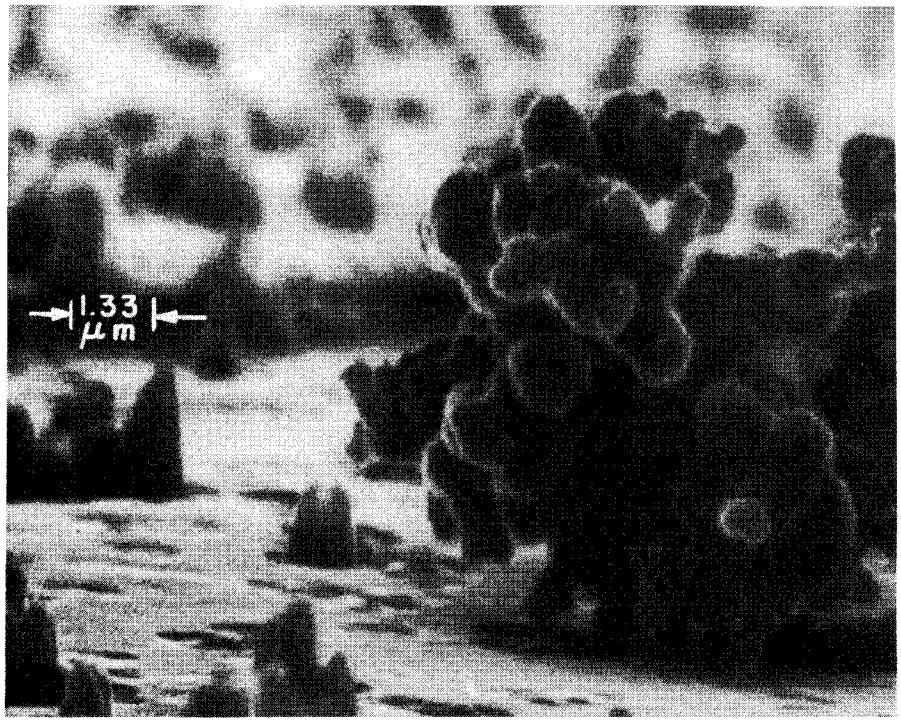

FIG. 6. PbS cluster on SiO_2–(100) Si (tilt angle: 60°).

etching, the spheres are seen to consist of the same size and shape crystallites as the PbS film.

The height of the cluster formations, on a thin PbS film (0.5 μm), varied typically between 1 and 3 μm as seen in Fig. 7. The cluster surface density measured on PbS-Si samples was typically 12% of surface area.

B. Substrate effect on crystallite orientation and size

Thin PbS films deposited on amorphous substrates do not show strong orientation.[29] However, it has been known that they can be grown epitaxially on such substrates as NaCl,[30,31] Ge,[6,32] and CdS [11] using a variety of techniques. As discussed above, PbS films solution grown on Si substrates are polycrystalline, with a grain size of approximately 0.25 μm. In this section we briefly review the effect of substrate orientation on the PbS crystallite orientation and size. A more detailed report is presented elsewhere.[33]

X-ray diffraction experiments were performed on a GE 11 GN1 diffractometer. A study of the diffraction pattern of

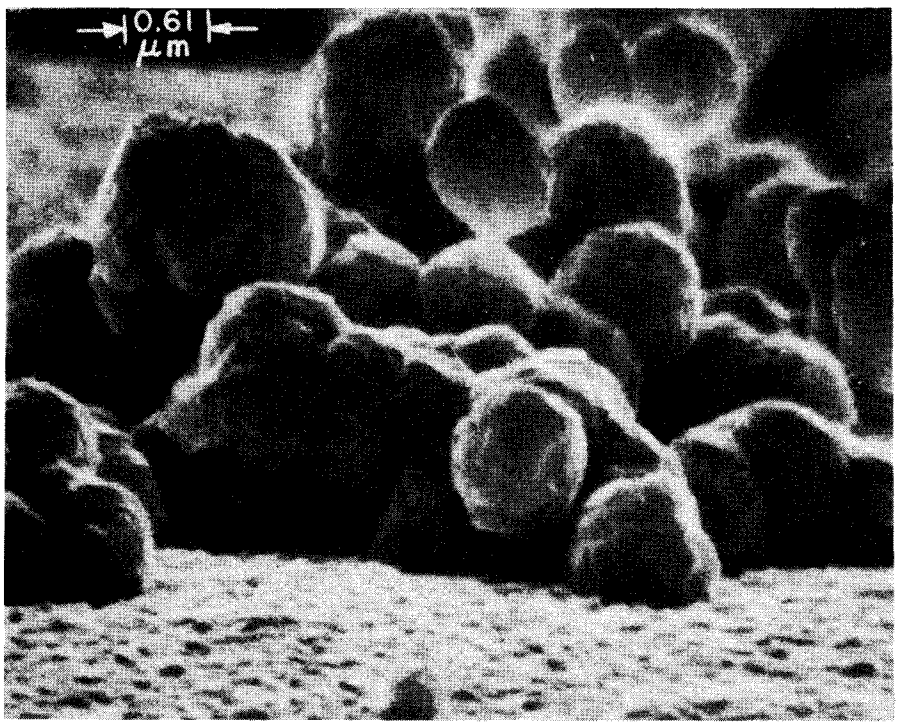

FIG. 7. PbS cluster on (100) Si after thermal etching, 200 °C, 20 h (tilt angle: 76°).

TABLE III. Tabulated diffraction data of a typical PbS-Si (100) heterojunction.

Diffraction pattern				PbS		Si	
Line	2Θ°	d (Å)[a]	I/I_0	d (Å)	I/I_0	d (Å)	I/I_0
1	26	3.43	0.54	3.429	6.25		
2	30.1	2.97	8.6	2.969	100		
3	42.6	2.12	0.65	2.099	7.5		
4	51	1.79	0.99	1.790	11.5		
5	53.5	1.71	0.11	1.714	1.25		
6	61.7[b]	1.50	2.5			1.35763[b]	2.5
7	62.6	1.48	0.3	1.484	3.5		
8	69.1	1.359	100			1.35763[c]	100
9	69.3[d]	1.355	53.3			1.35763[d]	53.3

[a]The angles are converted into a d value by the direct application of the Bragg Law, for λ (Å) = 1.54178.
[b]The diffraction line of d_{400} Si, corresponding to the CuK_β radiation.
[c]The diffraction line of d_{400} Si, corresponding to the CuK_{α_1} radiation.
[d]The diffraction line of d_{400} Si, corresponding to the CuK_{α_2} radiation.

the PbS-Si heterostructure shows that the pattern detected is that of a polycrystalline PbS film superimposed on the diffraction pattern of single-crystal silicon. The absence of any other diffraction patterns indicates that no other crystalline material, such as oxides of Pb and Si, exist with major ($> 1\%$) concentration in the heterostructure. However, it is not unlikely that impurities are present in trace amount but remain undetected by the x-ray analysis.

A tabulated diffraction pattern of a typical PbS-Si (100) heterojunctions is shown in Table III. The tabulation shows the measured 2Θ, twice the diffraction angle, the corresponding d values as computed form Bragg's law for the CuK_α line λ (Å) = 1.54178, the normalized intensity of the lines, and the corresponding PbS and Si diffraction patterns. The intensity distribution among the PbS diffraction lines shows that the intensity of the d_{200} line is an order of magnitude higher than any other diffraction intensity. This is evidence of a [100] preferential PbS crystallite orientation on Si (100) substrate: the PbS [100] axis is perpendicular to the plane of the Si (100) substrate and the crystallographic (200) plane of PbS is parallel to the Si (100) plane.

The minimum lattice mismatch between the cubic (100) planes of PbS and the (100) plane of Si crystal is 8.9%. The minimum mismatch corresponds to the case when the maximum distance between two silicon atoms on Si (100), which is the silicon lattice constant, is arranged to coincide with the interspacing of the cations (or anions) of PbS (100).

The diffraction data for PbS films grown on glass, (111) Si, and (100) Si (polished and unpolished) is tabulated in Table IV. The data presented here was measured on 4000-Å PbS film except for the sample prepared on unpolished Si, where the average thickness is 6000 Å. The tabulation shows the d values, the corresponding hkl indices, the 2Θ angle, and the relative intensity of the various diffraction lines. The data shown in Table IV for the PbS-Si on polished (100) substrate is the same on as in Table III and as discussed above the PbS exhibits a strong orientation in the (100) direction. Turning next to the PbS-Si (111), it is observed that the dominant lines are now the d_{220} and d_{311} . The PbS d_{200} line intensity in this case is undetermined due to a fluctuating unidentified substrate line. The x-ray diffraction data of PbS films grown on (111) Si and (100) Si is compared to that for powder sample in Fig. 8.

PbS grown on the amorphous glass substrate resembles the powder diffraction pattern with a very weak [100] preferential crystallite orientation similar to the results of Mirolyubov *et al.*[29] By comparing the relative intensities of the diffraction pattern of PbS grown on glass to that grown on (100) Si, it can be seen that a much smaller fraction of the crystallites grow in the [100] orientation in the former case.

PbS films grown on unpolished Si substrates exhibit an opaque cloudy appearance as opposed to the usual smooth mirrorlike finish seen on films grown on polished substrates. The diffraction pattern for these PbS films is seen in Table IV to be very close to that of PbS powder samples, indicating no preferred crystallite orientations.

TABLE IV. Tabulated diffraction data of PbS film grown on different substrates.

d (Å)	hkl	2Θ°	I/I_0, Galena[a] Powder sample	I/I_0, PbS-Si (100) Unpolished	Polished	I/I_0, PbS-Si (111)	I/I_0, PbS-glass
3.429	111	26.00	84	81.13	6.25	21.05	56.25
2.969	200	30.11	100	100	100	Undetermined	100
2.099	220	42.62	57	59.12	7.5	100	32.14
1.790	311	51.04	35	33.96	11.5	97.89	18.75
1.714	222	53.48	16	18.24	1.25	...	4.46
1.484	400	62.63	10	8.81	3.5	26.32	4.46
1.362	331	68.98	10	Undetermined		7.89	1.79
1.327	420	71.07	17	18.87	...	36.84	8.04
1.212	422	79.04	10	10.69	...	7.89	2.68
1.1424	511	84.92	6	6.60	...	13.16	...
1.0489	440	94.66	3	1.26	...	...	...
1.0034	531	100.46	5	3.77	...	...	...
0.9393	600	110.38	6	5.03	...	...	...
0.9386	620	110.51	4	4.09	...	...	...
0.9050	533	116.90	2	...	...	...	...
0.8952	622	118.97	4	...	...	...	...

[a]Diffraction data of the ASTM powder data file.

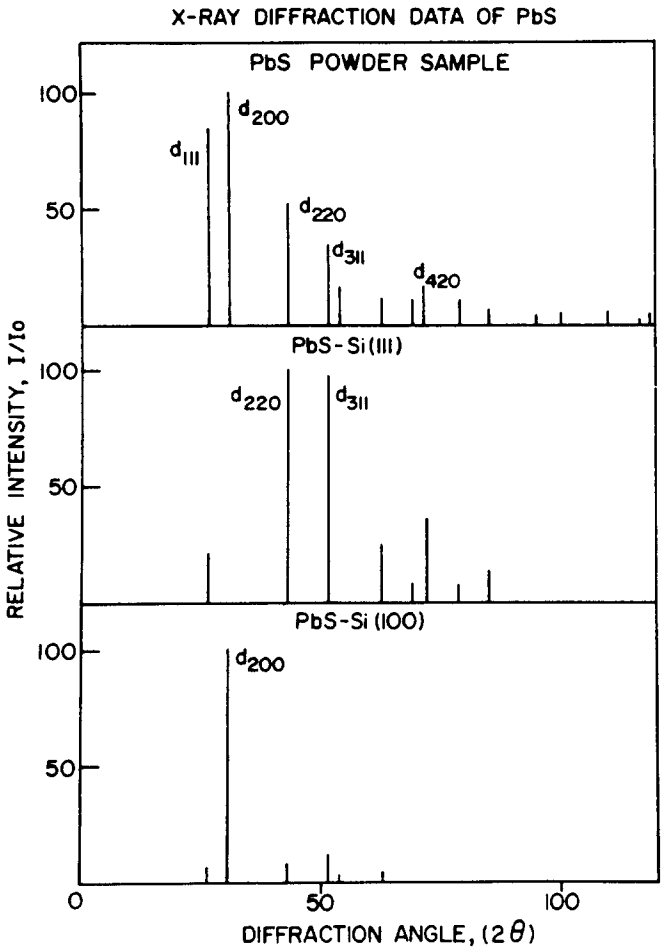

FIG. 8. X-ray diffraction data of PbS.

Laue back-reflection photographs for 2600-Å PbS films on (100) Si and (111) Si show the Si diffraction pattern superimposed on the Debye rings due to the PbS. The Debye rings are continuous and well defined, with little line broadening apparent, indicating a uniformly polycrystalline film.

The PbS mean crystallite dimension (D) can be evaluated from diffraction line broadening using the Scherrer equation[34]:

$$D = K\lambda / \beta \cos\Theta , \tag{1}$$

where Θ is the diffraction angle, λ is the wave length of the CuK_α radiation, and K is the shape factor which takes a value of about 0.9. β is the line broadening

$$\beta = B - b , \tag{2}$$

where B is the width of the PbS diffraction line at half-maximum intensity and b is the instrument effect estimated from the broadening of the single-crystal silicon diffraction line and corrected for the broadening caused by the K doublet.

The crystallite size of the PbS film as evaluated from the SEM picture in Sec. III A, is compared in Table II to the mean crystallite dimension (D) as computed from the x-ray line broadening. It should be pointed out that even though the estimate of grain size range from SEM photographs is not very accurate, the SEM and x-ray data are consistent. A larger grain size is observed in PbS film grown on (100) Si, as compared to that grown on (111) Si and glass substrates.

IV. PbS FILM AND HETEROJUNCTION CHEMICAL STRUCTURE

The chemical structures of the PbS film and of the PbS-Si interface were studied by the SEM/EDS technique and Auger electron spectroscopy (AES). The purpose of these studies was to (1) examine the uniformity of composition across the surface and along the depth of the film; (2) to compare the composition of the flat PbS film to that of the chainlike clusters appearing at the surface; (3) to determine the major contaminants at the surface and interface.

A. X-ray analysis of the chemical structure

An energy dispersive spectrometer (EDS)[35,36] was used in conjunction with SEM to obtain chemical information on the composition of the flat PbS film and the cluster macrostructure. The resolution, full width at one-half maximum

TABLE V. Results of SEM/EDS studies performed on the surface of PbS sample grown on glass substrate.

Peak (keV)	λ (Å)	I/I_0 Flat film	I/I_0 Cluster	λ (Å) Pb	S	Si	Transition
1.54	8.06	8.13	9.2				
				6.8			Pb$M_{\alpha_{1,2}}$
1.76	7.05	39.40	36.96				
						6.75	SiK_β
						7.12	Si$K_{\alpha_{1,2}}$
					5.37		S$K_{\alpha_{1,2}}$
2.32	5.35	100	100				
				5.2			Pb$M_{\alpha_{1,2}}$
				4.069			PbM_{III}
3.04	4.08	3.95	4.82				M_{III},$O_{IV,V}$
4.28	2.9	3.23	4.82				
7.66	1.62	1.25	1.90				
8.54	1.45	5.37	3.58	1.31			
10.48	1.18	11.38	11.86	1.18648			PbL_{α_2}
13.54	0.92	5.63	5.33	0.9268			PbL_{β_6}

TABLE VI. Results of SEM/EDS studies performed on the surfaces of PbS film and the cleaved surface natural galena.

Peak energy (keV)	Peak Wavelength (Å)	I/I_0 Galena	I/I_0 PbS film	Transition
1.76	7.05		34.90	$PbM_{\alpha_{1,2}}$
1.8	6.90	53.37		SiK_β
				$SiK_{\alpha_{1,2}}$
2.32	5.35		100	$SK_{\alpha_{1,2}}$
2.36	5.26	100		$PbM_{\alpha_{1,2}}$
2.98	4.17	96.92		$PbM_{III}O_I$
3.04	4.08		3.95	$PbM_{III}O_{IV,V}$
8.54	1.45		5.37	
8.60	1.44	52.14		
10.48	1.18	24.54	11.38	PbL_{α_1}
13.54	0.92		5.63	PbL_{β_1}

intensity of a spectral line (FWHM), is approximately 160 eV at 5.9 keV (Mn-K_α peak). At low energies the absorption effect in the beryllium (Be) entrance window dominates, making the detection of low-energy lines, such as oxygen, impossible.

Table V summarizes the results of SEM/EDS studies on the surface of PbS grown on glass. Data was taken at two different locations on the sample: at a point on the continuous film and on a relatively large cluster. The first entry in Table V notes the measured x-ray line followed by the corresponding wavelengths. The EDS data of the PbS sample is actually normalized to the coincident SK_{α_1} and K_{α_2} lines and the PbM_α peak occurring at 2.32 keV. The elemental transitions corresponding to each measured peak are listed in Siegbahn notation, together with the wavelength corresponding to the x-ray photon energy.

The electron scattering on rough surfaces, which limits the spatial resolution, is not a factor in the measurements made on the smooth and flat PbS film. In the semiquantitative evaluation of the cluster composition, Table V, the data presented is the average of repeated measurements carried out on several points on cluster macrostructures. The averaging process was used to avoid difficulties that can be encountered in the analysis when, due to backscattered electrons, much of the x radiation is excited by the surrounding film rather than the cluster. Cluster formations are sufficiently large, several microns, to allow locating the beam at different points on the same cluster. The difference in x-ray events accumulated at two different locations was usually no more than $\sim 5\%$ at any peak.

The EDS data shows close agreement between the energy of the lines experimentally observed and the theoretical value associated with the various Pb and S transitions. Furthermore, the relative intensity of the various lines for the continuous film and the cluster are within experimental error,[36] indicating a very similar chemical composition.

A comparison between the normalized EDS data measured on the PbS film and that measured on the surface of a cleaved natural galena crystal is shown in Table VI. Basically the same series of lines are detected in both cases leading to the conclusion that the chemical composition of the deposited PbS film is very similar to that of galena. The shift in peak energy for the various transitions was no more than 2%. In both cases the major transition was the 5.3-Å line. The only major discrepancy occurred in the relative intensity of the weaker lines. However, by examining the wavelength of the theoretical transitions in Table V, we can see that a number of experimental lines represent the continued effect of Pb, S, and Si transitions of nearly equal energy. One can therefore explain the slight energy shift and variation in relative intensity between deposited PbS and galena transitions as due to variations in the Pb : S ratio.

In addition to the peaks identified in Table VI, several other peaks associated with contamination in the natural galena crystal were detected. Zinc was identified, by the 1.44-Å and 1.283-Å lines, to be one of the contaminants present. Another wide and large peak exists below 1.6 keV. Poor resolution at this end of the scale prevented the identification of this line. It could be due to other contaminants and/or the result of x-rays excited in the instrument by backscattered electrons.

The EDS evaluation of the Pb : S peak ratio is not possible due to the overlap of the M_{α_1,α_2} line of lead and the K_{α_1} line of sulfur around 2.3 keV. To evaluate the sulfur and lead spearately, it would have been necessary to calibrate the ratio of M_α/L_α of Pb using a pure lead sample and use this ratio to calculate M_α–Pb and hence K_α–S. The Auger electron spectroscopy, however, is a direct and more accurate technique for the evaluation of the Pb : S ratio and of the presence of other peaks like oxygen.

B. Auger electron spectroscopy

The Auger electron spectroscopy technique was used to study in great detail a number of aspects of the PbS-Si heterojunction: Pb : S composition, interface width, surface and interface oxygen concentration, concentration profiles, multilayer films, heat-treatment effects, etc. The overall AES analysis is presented elsewhere.[37] However, in this paper the salient features related to the composition and structure of the PbS-Si HJ are summarized.

The Auger spectra of thin-film PbS chemically deposited on Si substrates were recorded. Since the Auger peak heights are proportional to the concentrations of the corresponding atomic species,[38] the relative intensities of the lead, Pb_{NOO}, and sulfur, S_{LMM}, Auger peaks were used to determine any change in surface composition. Depth-composition profiles of the PbS film and the PbS-Si interface are plotted from AES scans recorded while simultaneous ion sputter etching erodes the specimen surface. The depth-composition profiles are used to compare surface to bulk composition in PbS films and to study the width and composition in PbS-Si interface. Composition-depth profiles also provide information on the oxygen content of PbS prepared or treated under different conditions. The primary electron energy is 2.5 keV at total beam current of 20 μA. The beam diameter is 0.05–0.08 cm.

The composition depth profile of the PbS-Si HJ was

evaluated by monitoring the strongest peak of each element (Pb, S, Si) in the structure, while simultaneous ion sputter etching erodes the specimen surface. In the Auger spectrum of Pb, the strong peaks were contained in the 90–94 eV doublet, which can be associated with an *NOO* Auger transition. This poses a problem since the Si *KLL* transition at 92 eV, lies in close proximity to the Pb doublet. This prevented clear differentiation of the two elements at the interface. Therefore the Si_{LMM} line, at 1619 eV, and the Pb_{NOO} line, at 249–267 eV, had to be monitored for a meaningful evaluation of the position of the interface.

Prior to sputter etching PbS surface an oxygen peak is detected at 510 eV, as well as a number of other impurities. After approximately 5 min of sputter etching ($\sim$200 Å), the Auger spectrum of PbS is free of contamination and oxygen. The presence of oxygen at the surface of PbS layers was the subject of many investigations[38–43] and the amount of oxygen detected at the PbS film surface and PbS-Si interface showed considerable sensitivity to heat treatment.[87]

The composition depth profile of a 2000-Å PbS film grown on a (100) Si substrate is shown in Fig. 9. The elemental peaks are ploted in arbitrary units versus the ion bombardment time. The Ar ion beam current was set to 3 μA corresponding to a NiO etch rate of $\sim$ 10 Å/min. The depth resolution is estimated to be 10% of the overall etch depth. The PbS-Si interface is seen to coincide with the peak of an oxygen transition, O_{KLL}, profile. This effect has been consistently observed in all the Auger depth profiles.

The Pb and S peaks are seen to be constant in magnitude throughout the bulk of the film. This is taken as an indication of the homogeneity of composition through the film. The depth profile on Fig. 9 is typical for a PbS-Si HJ and is reproducible from sample to sample. The oxygen peak detected at the PbS-Si interface was about three times larger than that detected at the surface of the polycrystalline PbS film. However, this ratio varied from sample to sample and was also dependent on the post deposition treatment.[37]

No impurity peaks with the exception of oxygen were detected in the Auger spectra at the interface. This is taken as evidence of the absence of any chemical reaction between the chemical solution used in depositing PbS and the Si substrate. Hence, no significant insulative barriers consisting of other compounds are formed at the PbS-Si interface. This is an important result since it proves that an intimate contact between PbS and Si, a true heterojunction, can actually be formed by simple chemical deposition.

The presence of clusters, which are relatively large compared to the average film thickness, is probably responsible for the tailing of Pb and S peaks into the Si. The PbS-Si interface is defined to coincide with the peak of the O_{KLL} distribution.

The PbS-Si interface width determination is complicated by the different sputter yields and hence etch rates of its constituents.[37] A number of methods can be used to determine the interface width from the Auger depth profile: (a) extrapolation of the slopes of the main elements to their respective bulk value, (b) evaluation of sputter time required for the Si line to go from 20 to 80% of bulk value, (c) measurement of the full width of the oxygen peak at one-half of the maximum intensity, etc. Using a narrow 1-μm Auger beam and an etch rate based on SiO_2, the first method results in an interface width of 150 Å, while from the oxygen profile a value of 72 Å is obtained as shown in Fig. 10. Using the third method on the Si_{KLL} line results in an interface width of 83 Å. To obtain the "real" interface width from the measured values, corrections for the electron escape depth and the ion range are required.[44]

The ratio of the two main Auger transitions, S_{LMM} at 152 eV and Pb_{NOO} (Pb_1) at 90–94 eV, was used to detect changes in PbS compositions. The average $\langle S : Pb_1 \rangle$ ratio

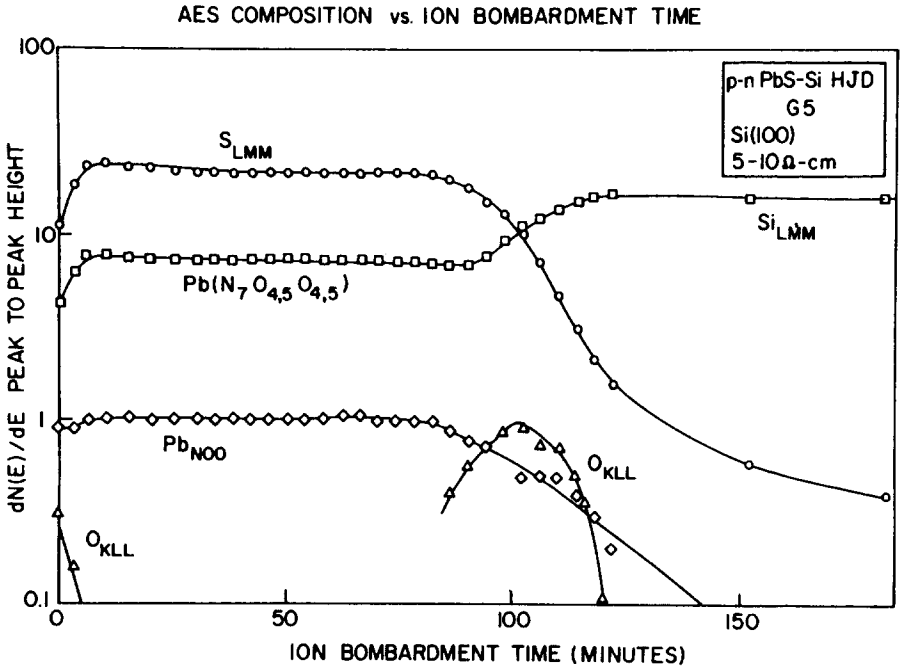

FIG. 9. AES composition versus ion bombardment time (G5).

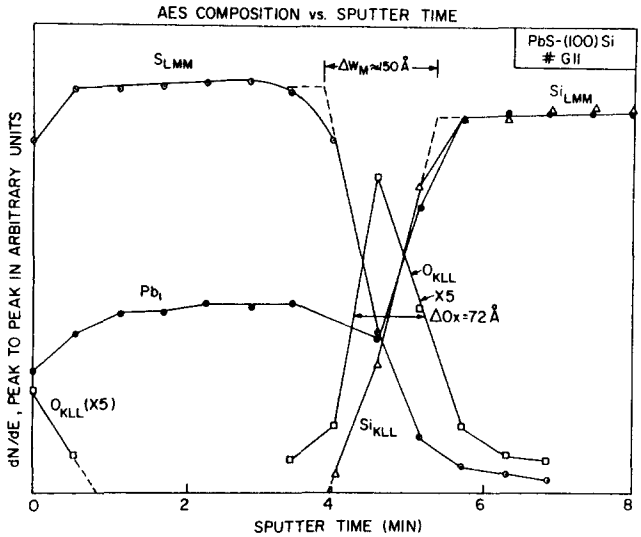

FIG. 10. AES composition versus sputter time (G11).

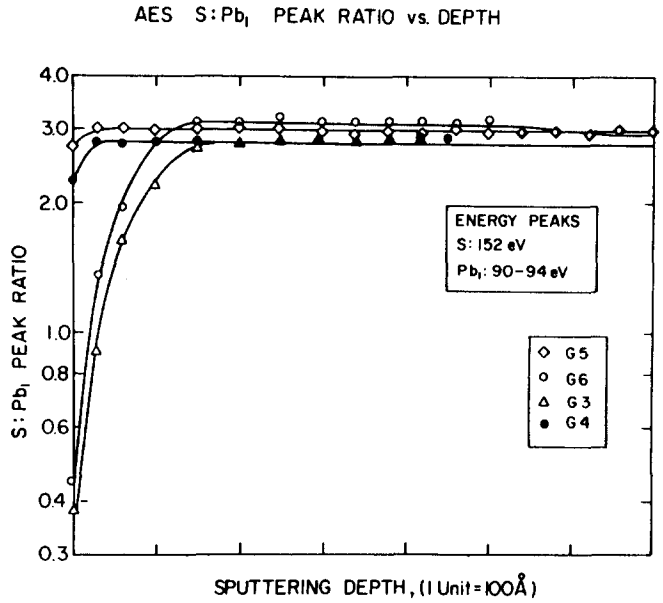

FIG. 11. AES S :Pb_I peak ratio versus depth.

measured for galena varied between 2.85 and 2.87 over a depth of 900 Å in three samples. The $\langle S : Pb_I \rangle$ ratio for galena can be taken as an estimate of the intensity ratio of those two peaks under stoichiometric conditions at a comparable surface roughness. The bulk $\langle S : Pb_I \rangle$ ratio for thin-film PbS samples varied from 2.8 to 3.0 when averaged over depth in seven samples. The deviation between the $\langle S : Pb_I \rangle$ ratio of the PbS films and galena samples is due to a combination of statistical error and the effect of surface roughness on the measurement. The resolution of the technique cannot account for the observed differences in the S : Pb ratio. To the extent to which this difference is real and due to nonstoichiometry, it will result in excess S atoms which can act as acceptors in the PbS films.

The PbS surface and PbS-Si interface were studied in some detail. A summary of the critical points are shown in Table VII. It can be seen from the tabulation that in a number of samples the surface composition of the PbS film differs substantially from that in the bulk, appearing Pb rich. The effect is most pronounced in samples G3 and G6 which were heated in air. Figure 11 illustrates this effect more clearly by plotting the $\langle S : Pb_I \rangle$ depth profiles of two PbS-Si samples heat treated in air (G3, G6), a third sample treated in N_2 ambient (G4), and a fourth sample which received no heat treatment (G5). It can be seen that heat treatment in air has a monotonically decreasing effect on the $\langle S : Pb_I \rangle$ ratio over the first 150 Å. Beyond this point the composition is basically the same in all samples and is uniform with depth. The decrease of the S : Pb ratio at the surface is attributed to the reduction of PbS by oxygen[40] resulting in the formation of lead and sulfur oxides. The increase in the interface O : S ratio with heat treatment is the result of a gettering effect.

TABLE VII. Surface, interface, and bulk composition from AES experiments.

Sample No.	Characteristics		$\langle S : Pb_I \rangle$[a] Surface Layer[c]	Bulk	$Pb_I : O$ Surface[d]	$S : O$[b] Surface[d]	Interface
G_1	PbS-glass		2.78	2.879	10.188	29.52	~1.00
G_2	Untreated		2.80	2.833	30.0	87.03	24.00
G_3	Air	PbS-Si	1.54	2.826	20.951	19.52	4.45
G_4	N_2	(111)	2.69	2.930	75.988	212.00	7.50
G_5	Untreated		2.99	3.023	41.339	125.99	12.2
G_6	Air	PbS-Si (100)	1.93	2.955	11.20	15.20	4.29
G_7	N_2		3.15	3.021	14.667	46.66	11.00

[a] S_{LMM} (152 eV) : Pb_{NOO} (90–94 eV).
[b] S_{LMM} (152 eV) : O_{KLL} (510 eV).
[c] Depth average over first 150 Å.
[d] Approximately 30 Å below surface.

VI. CONCLUSIONS

The PbS-Si HJ was fabricated by growing, at room temperature, a PbS film from chemical solution on a silicon substrate. It has been verified by AES that a direct and intimate contact between the two semiconductors is formed without any significant insulative barriers. The maximum PbS single film thickness obtained by this technique is approximately 0.6 μm. The as-grown PbS had a generally smooth appearance under the SEM. Chemical etching did not reveal the grain boundaries.

PbS films thermally etched at 200 °C showed a polycrystalline structure. The crystallite size was observed to vary between 0.2 and 0.4 μm depending on the substrate material and orientation. The mean crystallite dimension estimated from the line broadening of x-ray diffraction patterns was in agreement with the grain size evaluated from SEM analysis of the thermally etched samples. The favorite orientation of the PbS crystallites was (100) for Si (100) substrates. The diffraction pattern changed significantly for PbS on Si (111) substrates.

A secondary PbS macrostructure consisting of isolated chainlike clusters was found to coexist with the thin film. EDS analysis indicates that the clusters have the same chemical composition as the thin PbS film. The dimension of the clusters was generally up to an order of magnitude larger ($5\,\mu$m) than the thickness of the film ($<0.5\,\mu$m). The microstructure of the cluster, revealed by thermal etching, was found to be similar to that of the film, consisting of crystallites of the same size. No major contaminants appeared in the bulk or at the interface of the PbS-Si HJ. Minor oxygen peaks were detected by AES analysis at the surface of the PbS film and at the PbS-Si interface. The oxygen content increases substantially under long-term low-temperature heat treatment in air. The surface of thin-film PbS heat treated in air was generally enriched in lead.

[1]A.J. Steckl, IRIS Detector Meeting, 1977, p. 277, **127200-3-X**.
[2]A.J. Steckl, H. Elabd, and T. Jakobus, Tech. Digest IEDM, IEEE Cat. No. 77CH12757ED, 1977, p. 549.
[3]A.J. Steckl, M.E. Motamedi, and S.P. Sheu, Proc. IRIS, 1978, p. 401, **132900-4-X**.
[4]R.N. Lee, P.K. Scharnhorst, and R.B. Schoolar, NOLTR 73-213, 1974.
[5]A.J. Steckl, M.E. Motamedi, S.P. Sheu, H. Elabd, and K.Y. Tam, Proc. CCD '78 Conference, San Diego, 1978, p. 239 (unpublished).
[6]J.L. Davis and M.K. Norr, J. Appl. Phys. **37**, 1670 (1966).
[7]G. Guizzetti, F. Filippini, E. Reguzzoni, and G. Samoggia, Phys. Status Solidi A **6**, 605 (1971).
[8]N.I. Bochkareva, L.G. Paritskii, and S.M. Ryvkin, Sov. Phys. Semicond. **5**, (1971); **5**, 849 (1971).
[9]B.L. Sharma and S.N. Mukerjee, Phys. Status Solidi A **2**, K21 (1970).
[10]F. Bernabucci, G. Margarilondo, P. Migliorato, and P. Perfetti, Phys. Status Solidi A **15**, 621 (1973).
[11]Saburo Watanabe and Y. Mita, J. Electrochem. Soc. **116**, 989 (1969).
[12]Saburo Watanabe and Y. Mita, Solid-State Electron. **15**, 10 (1972).
[13]H. Sigmund and K. Berchtold, Phys. Status Solidi, **20**, 255 (1967).
[14]H. Rahnamai, Doctoral dissertation, University of Pennsylvania, 1976.
[15]H. Elabd and A.J. Steckl, J. Vac. Sci. Technol. **15**, 264 (1978).
[16]W. Kern and D.A. Puotinen, RCA Rev. **31**, 187 (1970).
[17]I.M. Kolthoff and P.J. Elving, *Treatise on Analytical Chemistry*, Part II, Sec. A (1962).
[18]F. Kicinski, Chem. Indus. **67**, 54 (1948).
[19]D.K. Smith, G.H. Blount, and R.T. Yamada, NTIS AD-A023 666-1, 1971.
[20]P.A. Buerger and O.A. Kunze, Int. IMEKO Symp. on Photon Detectors, 6th, Siofok, Hungary, 1974 (unpublished).
[21]D.E. Bode, *Physics of Thin Film, Advances in Research and Development* edited by G. Huss (Academic, New York, 1966), Vol. 3, p. 275.
[22]O.C. Wells, A. Boyde, and E. Lifshin, *Scanning Electron Microscopy*, (McGraw-Hill, New York, 1974).
[23]R.F. Brebrick and W.W. Scanlon, J. Chem. Phys. **27**, 607 (1957).
[24]K. Sangwal, Sov. Phys. Solid State **15**, 5 (1973); **15**, 943 (1973).
[25]W.M. Franklin and J.B. Wagnar, J. Appl. Phys. **34**, 3121 (1963).
[26]M.S. Seltzer, J. Appl. Phys. **37**, 4780 (1966).
[27]J.W. Mellor, *A Comprehensive Treatise on Inorganic and Theoretical Chemistry*, Longmans, Green & Co., London, 1927, p. 779.
[28]A.J.W. Moore, *Metal Surfaces, Structure-Energetics and Kinetics* (ASM, Philadelphia, 1962).
[29]V.R. Mirolyubov, G.A. Kitaev, and V.N. Dvoinin, Izv. Akad. Nauk SSSR Neorgan. Mater. **10**, 1761 (1975).
[30]R.V. Kudryavtseva and S.A. Semiletov, Sov. Phys. Crystallogr. **18**, 2 (1973); **18**, 272 (1973).
[31]G.I. Distler, S.A. Kolzareva, and Y.M. Gerasimov, Proceedings of the Second Colloquium on Thin Films, Budapest 1967, p. 81 (Vandenhoeck & Rupprecht Gottingen).
[32]M.S. Davydov, L.V. Degteva, A.I. Evanov, V.S. Kosnyrev, and G.R. Tikhomirov, Izv. Akad. Nauk SSSR Ser. Fiz. **36**, 1971 (1972).
[33]H. Elabd, A.J. Steckl, and W. Vidinski, Photovoltaic Device and Material Measurements Workshop, Arlington,Va. 1979 (unpublished).
[34]H.P. Klug and L.E. Alexander, *X-ray Diffraction Procedures for Polycrystalline and Amorphous Materials* (Wiley, New York, 1954).
[35]R. Woldseth, *X-ray Energy Spectrometry* (Kevex Corp., Burlingame, Calif., 1973).
[36]D.R. Beaman and J.A. Isasi, *Electron Beam Microanalysis* (ASTM, Philadelphia, 1972).
[37]H. Elabd and A.J. Steckl (unpublished).
[38]R.W. Weber and A.L. Johnson, J. Appl. Phys. **38**, 4355 (1967).
[39]L.J. Hillenbrand, J. Chem. Phys. **41**, 3971 (1964).
[40]L.J. Hillenbrand, J. Phys. Chem. **73**, 2902 (1969).
[41]R.N. Lee, J. Phys. (Paris) **29**, C4-43 (1968).
[42]Yu A. Zarif'yants and V.V. Kurylev, Sov. Phys. Semicond. **7**, 414 (1973).
[43]M. Sameh Said and J.N. Zemel, J. Appl. Phys. **47**, 866 (1976).
[44]J.S. Johannessen, W.E. Spicer, and Y.E. Strausser, J. Appl. Phys. **47**, 3028 (1976).